Cerebral Cortex August 2008;18:1758–1770
doi:10.1093/cercor/bhm199
Advance Access publication November 21, 2007

Cux-2 Controls the Proliferation of Neuronal Intermediate Precursors of the Cortical Subventricular Zone

Beatriz Cubelos[1,2], Alvaro Sebastián-Serrano[1], Seonhee Kim[3], Carmen Moreno-Ortiz[1], Juan Miguel Redondo[2], Christopher A. Walsh[3] and Marta Nieto[1]

[1]Centro Nacional de Biotecnología, CSIC, Darwin 3, Campus de Cantoblanco, Madrid 28049, Spain, [2]Fundación Centro Nacional de Investigaciones Cardiovasculares, Melchor Fenández Almagro 3, Madrid 28029, Spain and [3]Division of Genetics, Children's Hospital Boston and Howard Hughes Medical Institute, Beth Israel Deaconess Medical Center, Harvard Medical School, Boston, MA 02115, USA

Whereas neurons of the lower layers (VI–V) of the cerebral cortex are first born from dividing precursors at the ventricular zone, upper layer neurons (II–IV) subsequently arise from divisions of intermediate neuronal precursors at the subventricular zone (SVZ). Little is known about mechanisms that control the proliferation of SVZ neuronal precursors. We herein report that the restricted expression of the homeodomain transcription factor *Cux-2* in the SVZ regulates the proliferation of intermediate neuronal precursors and the number of upper layer neurons. In *Cux-2*-deficient mice (*Cux-2*−/−), there is excessive number of upper layer neurons and selective expansion of SVZ neuronal precursors. Double-labeling experiments demonstrate that *Cux-2*−/− upper layer precursors reenter the cell cycle in a higher frequency than wild-type precursors. Overexpression studies indicate that *Cux-2* controls cell cycle exit in a cell-autonomous manner. Analysis of *Cux-1*−/−; *Cux-2*−/− double mutant revealed that *Cux-2* controls SVZ proliferation independently of *Cux-1*, demonstrating that this is a unique function of *Cux-2*, not redundant with *Cux-1* activities. Our results point to *Cux-2* as a key element in the control of the proliferation rates of the SVZ precursors and the number of upper cortical neurons, without altering the number of deep cortical layers.

Keywords: cerebral cortex, *Cut*, *Cux-2*, late-born neurons, progenitor, transcription factor

Introduction

The vertebrate cortex is organized into distinct layers, with the neurons within each layer sharing similar functions, morphology, and birthdates. An important advance in the understanding of brain development is that we now know that the sequential birth of the distinct cortical layers is achieved via the generation of an intermediate neuronal precursor for the upper layers. Whereas neurons of the lower layers arise first from asymmetric divisions of the radial glial cells in the ventricular zone (VZ) (Malatesta et al. 2000; Noctor et al. 2001), neurons of the upper cortical layers are born from intermediate neuronal precursors dividing symmetrically in the subventricular zone (SVZ) (Haubensak et al. 2004; Miyata et al. 2004; Nieto et al. 2004; Noctor et al. 2004; Zimmer et al. 2004; Englund et al. 2005; Wu et al. 2005; Cappello et al. 2006). This 2-step mechanism of development has been proposed to confer an evolutionary advantage by enabling both the expansion of cortical layers and the appearance of new neuronal types (Englund et al. 2005; Gotz and Huttner 2005; Hill and Walsh 2005; Kriegstein et al. 2006).

Indeed, the evolution of the cerebral cortex extended the cortical surface area and increased the number of neuronal layers and neuronal circuits. Furthermore, the number of distinguishable upper layers increases from mice to humans (reviewed in Marin Padilla 2001) so that the circuit diagram differs between primates and other mammals (Hill and Walsh 2005).

Remarkably, this increment in the number of superficial layers of the cortex that occurs during evolution correlates with an expansion of the SVZ during embryonic development. This might be indeed attributable to an increase in the number of intermediate neuronal precursors. Furthermore, the selective expansion of the upper layers in the outer part of the cortical gyri and of their precursors at the SVZ has recently been proposed to contribute to the formation of the gyri typical of the cerebral cortex of carnivores and primates (Kriegstein et al. 2006).

Any account of the evolution and development of the cerebral cortex therefore requires an understanding of the molecular basis regulating the proliferation of SVZ precursors and differentiation of the upper layer neurons. Several molecules have been reported to control precursor cell proliferation (Takahashi et al. 1995; Chenn and Walsh 2002; Nowakowski et al. 2002), and the sequential activation of transcription factors governs the acquisition of specific laminar fates (Englund et al. 2005; Guillemot et al. 2006). However, little is known about factors involved in the selective proliferation and differentiation of SVZ precursors and upper layer neurons (Calegari et al. 2005; Guillemot et al. 2006; Glickstein et al. 2007). Genes selectively expressed in the neuronal precursor population of the SVZ during embryonic development, such as *SVET*, *Tbr-2*, *Nex/Math-2*, and *Cux-2* (Tarabykin et al. 2001; Nieto et al. 2004; Zimmer et al. 2004; Englund et al. 2005; Wu et al. 2005), may participate in these processes. Remarkably, 2 of these genes, *Cux-2* and *SVET*, are also expressed in the upper layer neurons.

Cux-2 encodes a vertebrate homolog of the Drosophila transcription factor *Cut* (Quaggin et al. 1996). In the peripheral nervous system, *Cut* determines the neuronal fate of external sensory organ precursor cells (Bodmer et al. 1987; Blochlinger et al. 1990) and the dendrite morphology of their neuronal progeny (Grueber et al. 2003). Upper layer neurons express *Cux-2* and a second *Cut* homolog, *Cux-1*, which does not show the same highly SVZ restricted expression during development (Nieto et al. 2004). The function of mammalian *Cux* genes in the nervous system is unknown. The overlapping expression patterns of *Cux-1* and *Cux-2* suggest redundant functions for these genes in neural cells and accordingly *Cux-1*-deficient mice (*Cux-1*−/−) show no specific phenotype related to the development of the nervous system (Luong et al. 2002). However, the restricted expression pattern of *Cux-2* in the

SVZ suggests specific functions for this transcription factor, possibly in the generation of neurons of the upper cortical layers. To address these issues, we generated a *Cux-2*-deficient mouse strain by targeted gene deletion and investigated the development of the cerebral cortex in these animals.

Our analysis of *Cux-2*–/– mice demonstrates that *Cux-2* negatively regulates the proliferation of precursors of the upper layer neurons in the SVZ, which reenter the cell cycle at a higher frequency in the *Cux-2*–/– mice. Thus, our results point to *Cux-2* as a gene, the expression of which limits the proliferation of SVZ intermediate precursor. In this context, mechanisms modulating *Cux-2* expression and functions appear to be candidate for playing important roles in the expansion of the cerebral cortex that occurs during evolution.

Experimental Procedures

Animals, Construction of a Mouse Cell Line Conditionally Targeting Cux-2/Cutl2, and Generation of Cux-2–/– Mice

All animal procedures were approved by the Centro Nacional de Biotecnología Animal Care and Use Committee, in compliance with National and European Legislation. *Cux-2* gene encodes 4 DNA-binding domains: 3 Cut repeats and 1 homeodomain. A targeting construct was designed to conditionally eliminate exons 22 and 23, which encode the third Cut repeat and part of the homeodomain (exons 22 and 23) near the C terminus of the Cux-2 protein, and to create a premature stop codon 3′ after the deletion. The targeting vector was constructed using a 1.9-kb DNA fragment that contains regions located 1.4 kb 5′ and 0.5 kb 3′ of exon 21. The middle arm, containing exons 22 and 23, is a 1.7-kb polymerase chain reaction (PCR) product. The long arm is a 7.5-kb NdeI genomic fragment from a mouse lambda library. A total of 10 μg of targeting vector was linearized with NotI and then transfected into J1-129 embryonic stem cells by electroporation. After selection in G418, surviving colonies were expanded and analyzed by Southern blot to identify clones that had undergone homologous recombination. Correctly, targeted ES cell lines were microinjected into C57BL/6J blastocysts. Resulting chimeric mice were crossed with C57BL6 mice to obtain *Cux-2+/loxP* mice. Mice carrying the conditional allele (*Cux2loxP*) were mated with mice expressing CRE recombinase under the human beta-actin promoter (Tg (ACTB-CRE)2Mrt deleter mice; Jackson Laboratories, Bar Harbor, ME) on a Swiss Webster background, to obtain mice giving germ line transmission of the floxed null allele. Heterozygous (het) mice for this allele (hereafter *Cux-2+/–*) were crossed with wild-type (WT) mice to segregate from the beta-actin transgene. *Cux-2+/–* animals were mated to obtain *Cux-2* homozygous mutant mice (*Cux-2–/–*). Previous studies with antibodies that recognize different regions of the Cux-2 protein have found 2 isoforms of Cux-2 protein in a human cell line. Both isoforms are recognized by an antibody against the N-terminal part of the protein (anti-Cux-2 antibody 356) encoded by the undeleted part of the targeted Cux-2 gene. Anti-Cux-2 antibody 356 shows immunoreactivity with mouse Cux-2 (Gingras et al. 2005). Western blot analysis of the expression of Cux-2 protein in *Cux-2*–/– mice using antibody 356 reveals 2 bands in adult cerebral cortex homogenates (Supplementary Fig. 1). No bands were detected on brain homogenates from adult *Cux-2*–/– animals (Supplementary Fig. 1). Immunohistochemistry (IHC) studies using antibody 356 shows expression of Cux-2 protein in the WT brains but not in *Cux-2*–/– animals. These experiments demonstrate the complete absence of Cux-2 protein and lack of Cux-2 truncated mutated forms of the protein in the *Cux-2*–/– animals. *Cux-1*–/– mice have been described previously (Luong et al. 2002) and were obtained from A. J. van Wijnen (University of Massachusetts Medical School, MA, USA). Animals were maintained on a C57BL6: Swiss Webster background. Morning of the day of the appearance of the vaginal plug was defined as embryonic day (E) 0.5.

Southern Blot and PCR

Genomic DNA was obtained from ES cell clones or tail biopsies and digested with KpnI. Southern blot was performed using ExpressHyb hybridization solution (BD Biosciences, Mountain View, CA) according to the manufacturer's protocol. A 1-kb cDNA probe corresponding to exon 24 was used to screen for positive ES cell clones and to genotype mice carrying the *loxP* and null alleles. Mice were screened by Southern blot and the PCR. Primers for the detection of the null floxed allele were 5′-AAGGGCGGTGATTACAGAGA-3′ and 5′-GCCTGCTGTGGTAGACAGGT-3′; primers for the WT allele were 5′-TCAGCACATGGTGTCTGGAT-3′and 5′-CCTACTTTCTGCCTGCTTG-3′. PCR was carried out over 35 cycles of 94 °C for 1 min, 60 °C for 1 min, and 72 °C for 1 min in 2.5 mM Mg2Cl and 5 mM Betaine.

Antibodies, IHC, and Histology

Mice were perfused transcardially with 0.1 M phosphate-buffered saline (PBS; pH 7.4) followed by cold 4% paraformaldehyde in PBS. The perfused brains were removed and postfixed in 4% paraformaldehyde at 4 °C overnight. Fixed brains were cryoprotected in 30% sucrose in PBS and sectioned on a cryostat to produce either 10–20 μM cryosections on Superfrost Plus microscope slides (Fisher Scientific, Pittsburgh, PA) or 50–100 μM floating cryosections. Sections were blocked for 1 h at room temperature (r.t.) with 5% horse serum in PBS containing 0.5% Triton-X 100 (blocking solution) and then incubated for 1 h at r.t. or overnight at 4 °C with primary antibodies diluted in blocking solution. Fluorescent-tagged secondary antibodies (in PBS, 5% horse serum) were applied for 1 h at r.t., and sections were counterstained with Hoechst 33342 (Molecular Probes, Eugene, OR) and mounted in Aqua-polymount mounting medium (Poly-Labo, Strasbourg, France). Peroxidase/diaminobenzidine IHC staining was performed as described (Cubelos et al. 2005). Briefly, after incubation with primary antibody, sections were incubated with biotinylated donkey anti-rabbit IgG (Sigma, St Louis, MO) for 1 h. Sections were then washed 3 times in PBS, incubated with streptavidin-biotinylated horseradish peroxidase complex, washed, and incubated with 0.1 mg/ml H_2O_2 and 0.5 mg/mL diaminobenzidine in PBS. Sections were mounted in glycerol–gelatin.

The following primary antibodies were used at the dilutions indicated: rabbit polyclonal anti-Cux-1 (clone M222) (1:10) and anti-Brn-1 (1:50) (Santa Cruz Biotechnologies Inc., St Cruz, CA), rabbit polyclonal antiphosphohistone H3 (pH3) (1:500) (Upstate, Spartanburg, SC), rabbit anticleaved caspase-3 (1:500) (Cell Signaling Tech Inc., Danuers, MA), rabbit anti Ki67 (Novocastra, Newcastle on Tyne, UK), rabbit polyclonal anti-Cux-2 (antibody 356, a gift from Dr Alex Nepveu of McGill University Health Centre, Canada), rat anti-bromodeoxiuridine (BrdU) (1:50) (BD Biosciences), and rabbit anti-Tbr-2 antibody

(1:500) (Chemicon Inc., Hampshire, UK). Goat anti-rabbit and goat anti-rabbit and anti-mouse secondary antibodies, conjugated to Alexa 488 and 594, respectively (Molecular Probes), were applied at 1:500. Before staining for Cux-1, Cux-2, Ki67, BrdU, clorodeoxiuridine (CldU), iododeoxiuridine (IdU), or pH3, sections were boiled for 30 min in antigen retrieval solution (Vector Laboratories, Burlingame, CA). This was followed in the case of staining for BrdU, CldU, IdU, and pH3 by 30-min treatment with 2 N HCl.

Staining for CldU and IdU was performed as described (Aten et al. 1994). Briefly, slides were incubated overnight at 4 °C with a mouse monoclonal anti-BrdU antibody (1:50; BD Biosciences; cross-reactivity with IdU), then washed in Tris buffer, pH 8.0, containing 0.5 M NaCl and 1% Tween 20 for 20 min at r.t. to eliminate background and possible cross-reactivity with CldU, and incubated overnight at 4 °C with rat monoclonal anti-BrdU antibodies (1:250; Abcam, Cambridge, UK; cross-reactivity with CldU). Secondary anti-mouse conjugated to Alexa 495–conjugated and anti-rat Alexa 598–conjugated antibodies (1:500; both from Molecular Probes) were applied for 2 h at r.t. The presence of single positive neurons for IdU and CldU in the stained cortical sections demonstrated the specificity of the antibodies and the staining.

BrdU, CldU, and IdU Injections and Cell Counting

All BrdU, CldU, and IdU quantification analysis show results obtained from the primary sensory cortex (primary somatosensory cortex barrel field [S1BF]. Interaural 2.34-2.22, Bregma 1.46-1.58 according to the mouse atlas of Paxinos and Franklin 1997). Similar results were observed in the primary motor cortex and other regions of the sensory cortex (M1 and primary somatosensory cortex forelimb region [S1FL], according to the mouse atlas of Paxinos and Franklin). BrdU, IdU, and CldU were administered intraperitoneally at 5 mg/mL in PBS. A single CldU injection was given 10 h after IdU injection at E14.5. Anatomically matched sections were selected from each mouse at each stage after BrdU injection ($n = 3$ *Cux-2*+/*?* control mice and $n = 3$ *Cux-2*–/– mice), and BrdU was detected by IHC. The total cortical thickness was subdivided into 10 bins of equal area, and the number of cells in which at least half of the nucleus was BrdU positive was counted in each bin. Identical results were obtained from independent analyses by 2 investigators.

Cortical Layer Thickness and Neuronal Density

For neuronal cell density and cortical thickness, serial sections were cut from brains of control and *Cux-2*–/– animal ($n = 3$). Then sections were Nissl stained, matched, and photographed. Measurements and cell counts were performed on the primary sensory cortex (S1BF, Interaural 2.34-2.22, Bregma 1.46-1.58 according to the mouse atlas of Paxinos and Franklin 1997). Similar results of increased layer thickness were observed in S1FL and M1 (Paxinos and Franklin 1997). Analysis was performed blind by 2 investigators in independent analyses. Cell density was calculated using the optical fractionator method (Sterio 1984). Optical dissector was given by a preexisting microscope grid ($x, y, z = 61, 61, 10$ μm). For cortical thickness, 4–5 measurements were taken of each brain region and mean values and standard deviations obtained. Statistical significance was calculated using the 2-tailed Student's *t*-test.

Confocal Microscopy and Imaging

Confocal microscopy was performed with a Radiance 2100 (Bio-Rad, Hercules, CA) Laser Scanning System on a Zeiss Axiovert 200 microscope. For fluorescence excitation, an argon ion laser (488 nm), a Krypton–Neon laser (543 nm), and a red diode (637 nm) were employed. The filter combinations used for detection of Alexa 488 and Alexa 594 were a 560 DCLPXR beam splitter and HQ 515/30 emission filter and a 650 DCLPXR beam splitter with HQ 590/70, respectively. Sequential images were taken with LaserSharp v5.0 software (Bio-Rad) and analyzed using LaserPix v.4 image software (Bio-Rad).

Neurosphere Culture, Nucleofection, and Constructs

Dorsal telencephalons of E14.5 WT embryos were dissected and cells dissociated as described (Nieto et al. 2004). Dissociated single cells were cultured in DMEM-F12 supplemented with N2, fibroblast growth factor (10 ng/mL), and epidermal growth factor (10 ng/mL) (Gibco, Invitrogen, Carlsbad, CA). Neurosphere cultures were passaged every 3 days by mechanical dissociation. Dissociated cells were cotransfected using the nucleofector technic (Amaxa Biosystems, Gaithersburg, MD) with 2.5 μg each of DNA constructs containing *Cux-2* and green fluorescence protein (GFP) cDNAs under the cytomegalovirus enhancer, chicken β-actin promoter, and rabbit β-globin poly(A) signal (CAG) (cytomegalovirus [CMV] and beta-actin) promoter or the empty vector and GFP construct. Neurosphere formation was monitored after 10 days in culture.

Results

Generation of Cux-2–/– Mice

To investigate the functions of *Cux-2* in the development of the nervous system, we generated mice carrying a null allele of *Cux-2* and analyzed the resulting brain phenotype. The mutation was designed to remove exons 22–23 that encode the third Cut repeat and the homeodomain near the C-terminal end of the protein. Het *Cux-2*+/– mice were obtained by breeding mice carrying a *Cux-2* conditional allele (*Cux-2*+/*loxP*) with CRE deleter mice (see Experimental Procedure and Fig. 1*a–c*). Homozygous *Cux-2* mutant mice (*Cux-2*–/–) were obtained by crossing het *Cux-2*+/– animals. *Cux-2*–/– mice were born at the expected Mendelian ratios and showed overall normal development and growth (not shown). To confirm that the mutation of the Cux-2 C terminus effectively removed expression of Cux-2 protein in mutant mice, postnatal brain sections of WT and *Cux-2*–/– mice were stained with a Cux-2 antiserum against the N-terminal part of the protein that recognizes the 2 described isoforms of Cux-2 protein but does not recognize Cux-1 (Gingras et al. 2005). This demonstrated the complete absence of Cux-2 immunoreactivity in all brain regions of *Cux-2*–/– animals, including the upper layer neurons and neurons of the ventrolateral and piriform cortex (Fig. 1*d*, left panels). Western blot experiments confirmed the complete absence of Cux-2 protein in *Cux-2*–/– cortical homogenates (Supplementary Fig. 1). In contrast, staining with a Cux-1-specific antiserum showed that the Cux-1 protein expression was indistinguishable between *Cux-2*–/–, *Cux-2*+/–, and WT littermates (Fig. 1*d* and not shown). Thus, loss of Cux-2 protein expression does not affect the expression

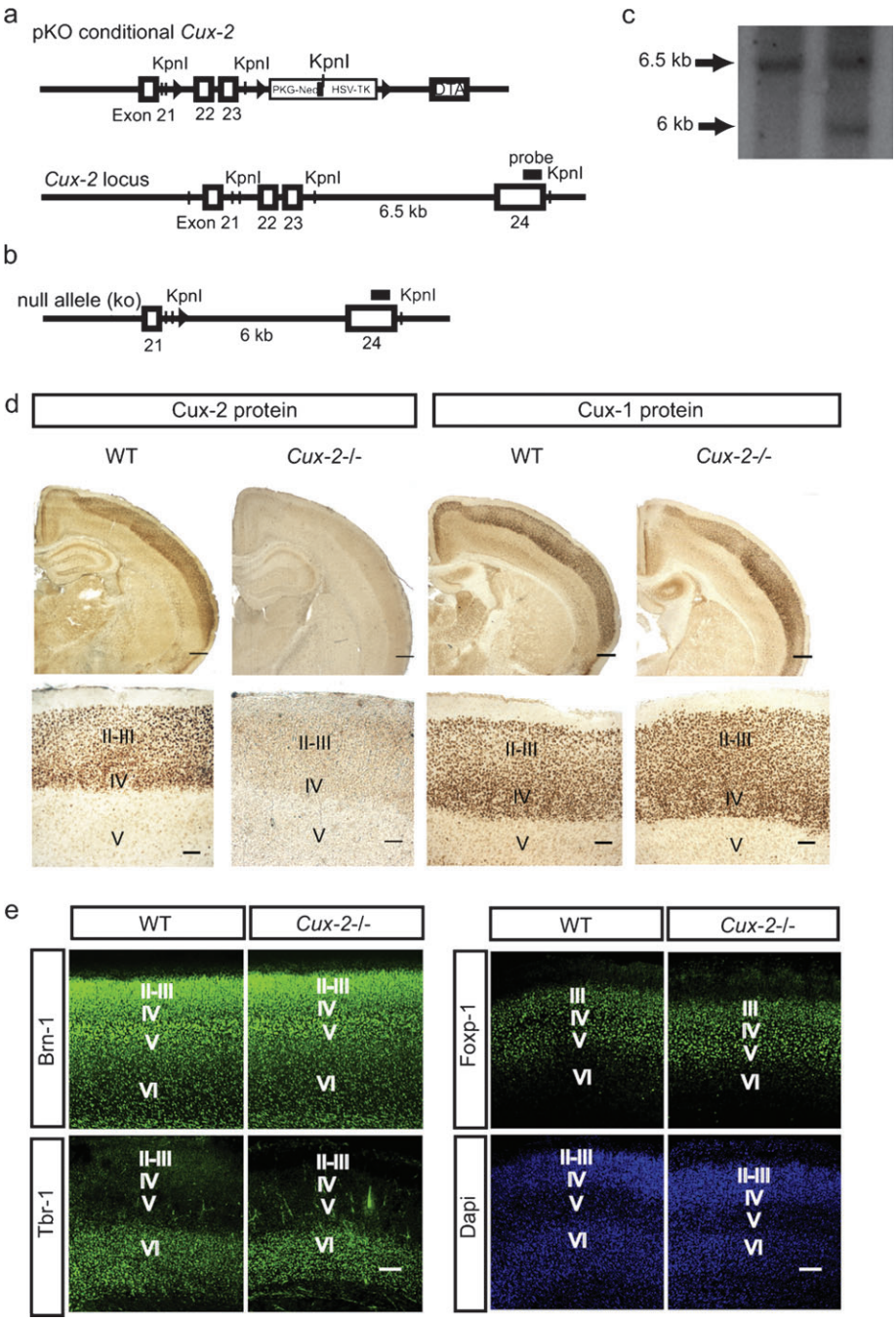

Figure 1. Targeting strategy for *Cux-2* null mutation. (*a*) A Neo-TK cassette flanked by loxP sites (black arrowheads) was inserted downstream of a 1.5-kb fragment containing *Cux-2* exons 22 and 23. A third loxP site was introduced 1-kb upstream of exon 22. *Cux-2+/loxP* het mice were bred with mice expressing CRE recombinase under the human beta-actin promoter to obtain mice bearing the floxed null allele (*Cux-2* allele) (*b*). (*c*) Southern analysis of the null mutation in the germ line. The Southern blot probe used is a 500-bp fragment of exon 24 (panels a and b). (*d*) Expression of Cux-2 and Cux-1 protein in the WT and *Cux-2−/−* cortex. Expression of Cux-2 protein was undetectable in all regions of the *Cux-2−/−* P21 mutant telencephalon, including the upper layers of the cortex (left, lower panels). Cux-1 protein expression was indistinguishable between WT and *Cux-2−/−* homozygous P21 mutant mice (right). Bars represent 500 μm (upper panels) and 100 μm (lower panels). (*e*) Expression of layer-specific markers in the telencephalon of P0 WT and *Cux-2−/−* mice. Bars represent 100 μm.

of Cux-1. Also unaffected were the expression patterns of the layer-specific transcription factors, Brn-1 (II-V), Foxp-1 (III–V), Id-2 (II, III, V, and VI), and Tbr-1 (VI) (Bulfone et al. 1995; Rubenstein et al. 1999; Hevner et al. 2001; McEvilly et al. 2002; Sugitani et al. 2002; Ferland et al. 2003) (Fig. 1*e*). These results thus show that in mice completely lacking Cux-2 protein expression, upper and lower layer neurons each acquire their correct laminar position and correctly expressed the early layer-specific markers that we analyzed.

Cell Density and Total Neuronal Numbers Are Increased in the Upper Layers of the Cux-2−/− Cerebral Cortex

Visual analysis indicated that adult *Cux-2−/−* brains were moderately but consistently bigger in volume than WT brains

(Fig. 2*a*). Examination of histological sections showed that both cell density and the thickness of upper cortical layers (II–IV) of *Cux-2–/–* mice was greater than in WT animals (Fig. 2*b,c*). The increased cell density was significant in layers II–III, (20% increment) but was most pronounced in layer IV (30% increment). In contrast, we observed no differences in neuronal density in layers V and VI (Fig. 2*b*). The increased cell density in the *Cux-2–/–* upper layers was accompanied by a moderate increase in the thickness of upper layers (15% increment) (Fig. 2*c*). Again, this increment was not observed in lower layers and resulted in a modest increase in the overall cortical thickness (Fig. 2*c*). The combination of increased cellular density and increased upper layer cortical thickness indicates an important increase in the total number of neurons in layers II–III and IV of the *Cux-2–/–* cortex.

BrdU birthdating experiments performed at E13.5, E14.5, and E16.5 (Fig. 3) confirmed the selective increase in the number of upper layer neurons. In accordance with the correct expression of layer-specific markers (Fig. 1*e*), the BrdU experiments suggested normal neuronal migration: neurons born at E14.5 and E16.5 populated the upper part of the postnatal cortex (P21) and not the deep cortex in control and *Cux-2–/–* animals (Fig. 3*a–c*). Likewise, neurons born at E13.5 populated the deep cortical layers in both groups of mice (Fig. 3*d*). However, the number of BrdU-positive neurons that populated the superficial bins of *Cux-2–/–* animals and that were born at E14.5 and E16.5 was increased 40% and 30%, respectively, in *Cux-2–/–* mice compared with control mice (WT or *Cux-2+/–*) (Fig. 3*b,c*, bins 2–4 at E16.5 and bins 2–5 at E14.5). In contrasts, no differences were found between the populations born at E13.5 (Fig. 3*c*). Interestingly, the increased number of labeled upper layer neurons was produced by an increase in the number of dimly fluorescent BrdU–labeled cells (Fig. 3*a–c*, right panels), suggesting that the pulse label had been diluted by additional rounds of cell division. Hence, upper layer precursors appear to undergo additional rounds of division when *Cux-2* is removed. Also supporting an increase in proliferation, the rates of apoptosis in the brains of WT and *Cux-2–/–* mice at P0 and P16 postnatal stages were the same (Fig. 4*a,b*). Thus, the increment in the number of upper layer neurons in the *Cux-2–/–* mice cannot be attributed to defective neuronal apoptosis. Decreased postnatal apoptosis in *Cux-2–/–* mice would also predict less significant differences in the number of BrdU-labeled upper layer neurons at early postnatal stages than in the late postnatal days. But we found increased numbers of E16.5 BrdU–labeled neuronal population in the *Cux-2–/–* cortex already at the first postnatal days (P0–P5), and the increment was equivalent to that found at P21 (Fig. 4*c* and see also Fig. 6). All together, we conclude that the increase number of upper layer neurons in the *Cux-2–/–* mutant mice is due to increased proliferation of neuronal precursors during development and not to decreased apoptosis.

Neuronal Proliferation Is Increased in the SVZ of Cux-2 Mutant Mice

The restricted expression of *Cux-2* mRNA (Nieto et al. 2004) and protein in the SVZ (Supplementary Fig. 2) and the increased upper layer neurons in *Cux-2–/–* mice suggest that *Cux-2* has specific functions in the proliferation of intermediate precursors for upper layer neurons. To identify possible differences in cell cycle parameters, we combined immunostaining for Ki67 antigen, a protein expressed in all dividing cells, and a pulse of

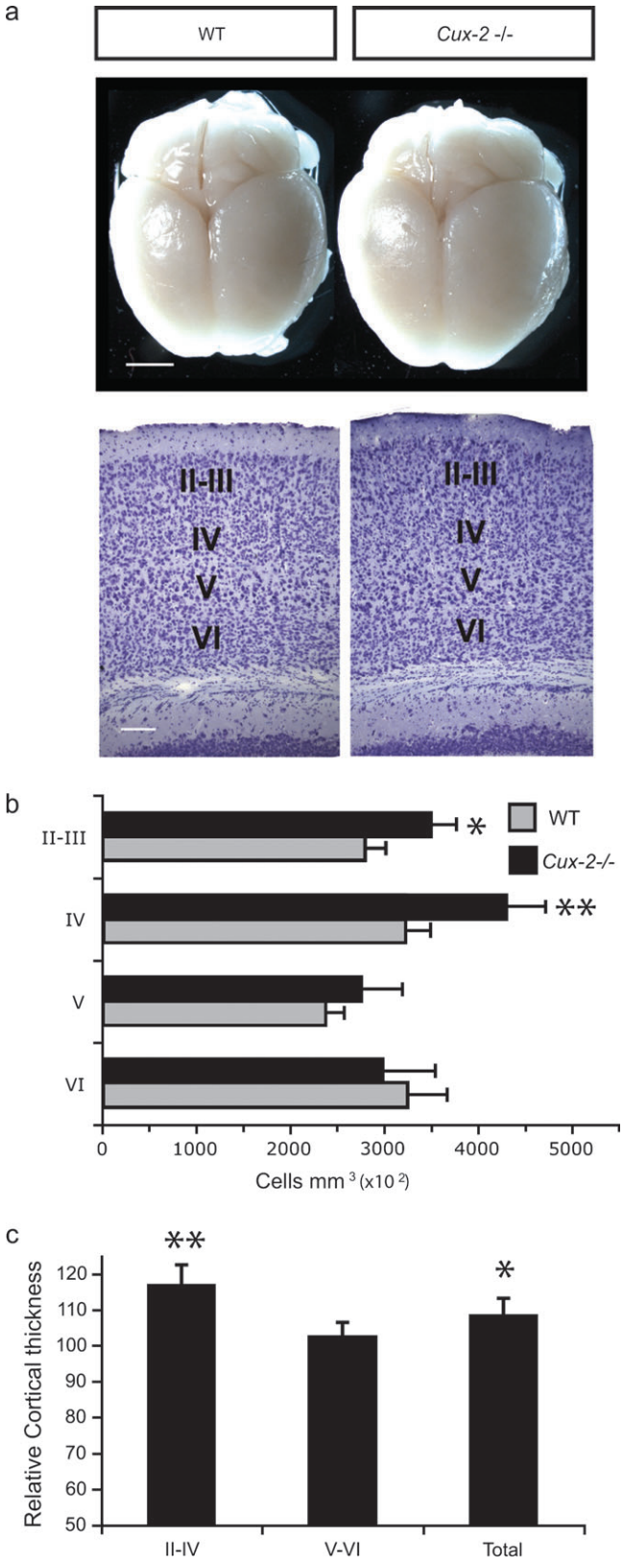

Figure 2. Cell density and thickness of cortical layers in the adult WT and *Cux-2–/–* cortex. (*a*) Brains of WT and *Cux-2–/–* animals (upper panel). Nissl staining of cortices from WT and *Cux-2–/–* adult mice. Bar represents 100 μm. (*b*) Cell density in each cortical layer of *Cux-2–/–* and WT mice. (*c*) Average thickness of the total cortex and of each layer in the *Cux-2–/–* adult animals relative to measures taken in the adult WT cortex. $^{*}P < 0.05$, $^{**}P < 0.01$ between WT and mutant cortex.

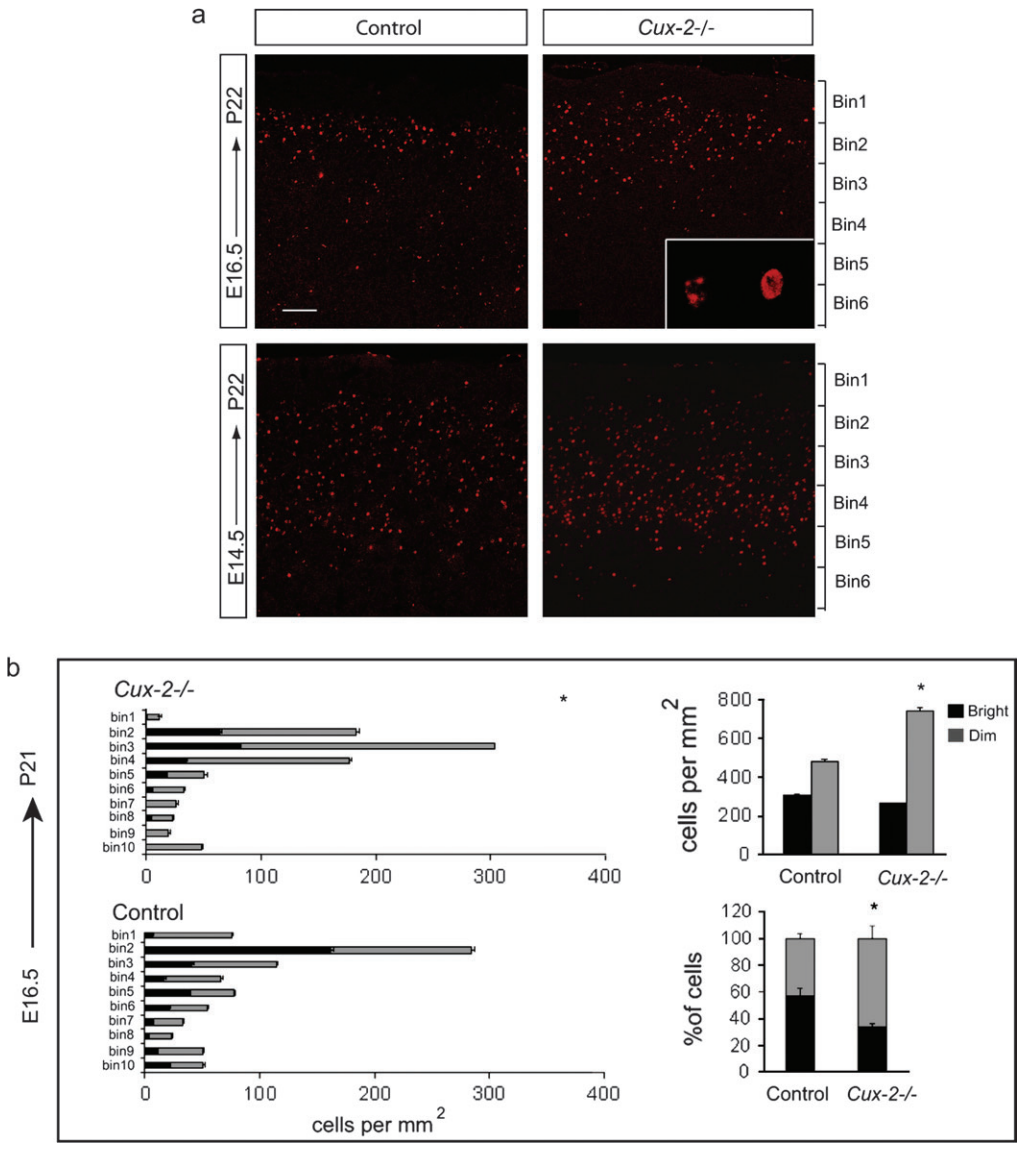

Figure 3. BrdU birthdating experiments of *Cux-2−/−* cortical neurons. (*a*) Representative micrographs of cortical sections taken at P21 showing neurons labeled by BrdU injection at E16.5 (upper panels) and E14.5 (lower panels) in control (*Cux-2+/?)* and *Cux-2*-deficient (*Cux-2−/−*) mice. Bar represents 100 μm. The division of the cortex into equal-sized bins is shown on the right. Inset shows representative examples of bright and dim BrdU-stained nuclei. Quantitative analysis of the distribution of BrdU populations labeled at E16.5 (*b*), E14.5 (*c*), and E13.5 (*d*) and examined at P21. Black and gray bars represent bright and dim BrdU-stained nuclei, respectively. The left-hand charts show the distribution of BrdU-labeled cells in each of 10 equal bins dividing the cortex. $^*P < 0.01$ as analyzed by a 10×2 chi-square matrix test. The upper right-hand charts show the total number of cells labeled in all sections of control and *Cux-2−/−* mice. Lower right charts show the relative proportion of dark and dim BrdU-stained nuclei. $^*P < 0.01$ as analyzed by 2-tailed Student's *t*-test.

BrdU to label cells in the S phase. After a 2-h pulse of BrdU in E15.5 embryos, precursor cells in the SVZ were identified as those set apart from the BrdU-positive precursors aligned along the VZ (Fig. 5*a*). Remarkably, the number of Ki67- and BrdU-positive cells was dramatically increased in the SVZ of *Cux-2–/–* cortex (Fig. 5*a*, left panel graph). No significant differences were observed in the proportion of cycling cells that were in the S phase (i.e., the ratio of BrdU+/Ki67+) between the control and *Cux-2–/–* mutant mice. Because this ratio provides an estimate of cell cycle length, this therefore indicates that *Cux-2–/–* and control SVZ precursors cycled at similar rates (Fig. 5*a*, right panel graph).

We next studied the number and location of cells undergoing mitosis with an antibody against the phosphorylated form of histone 3 (pH3). pH3 staining of E15.5 cortical sections revealed 2 mitotic zones: apical mitosis occurring in radial glial cells at the ventricular walls and basal mitosis, clearly separated from the ventricle, occurring in cycling cells of the SVZ (Fig. 5*b*). Quantification analysis revealed that the number of cells in basal mitosis was greatly increased in the SVZ of E15.5 *Cux-2–/–* mice compared with their WT counterparts (Fig. 5*b*, graph). In contrast, no differences were observed in numbers of cells undergoing apical mitosis (Fig. 5*b*, graph). This indicates that proliferation of VZ precursors, which do not express *Cux-2*, is not affected in *Cux-2–/–* mice and demonstrates a selective increase in the proliferation of SVZ neuronal precursors but not of radial glial cells. In agreement with this, the number of Tbr-2 positive cells, which mark intermediate neuronal progenitors in the proliferative regions (Englund et al. 2005), was dramatically increased in the cortex of *Cux-2–/–* mice (Fig. 5*c*). Similarly,

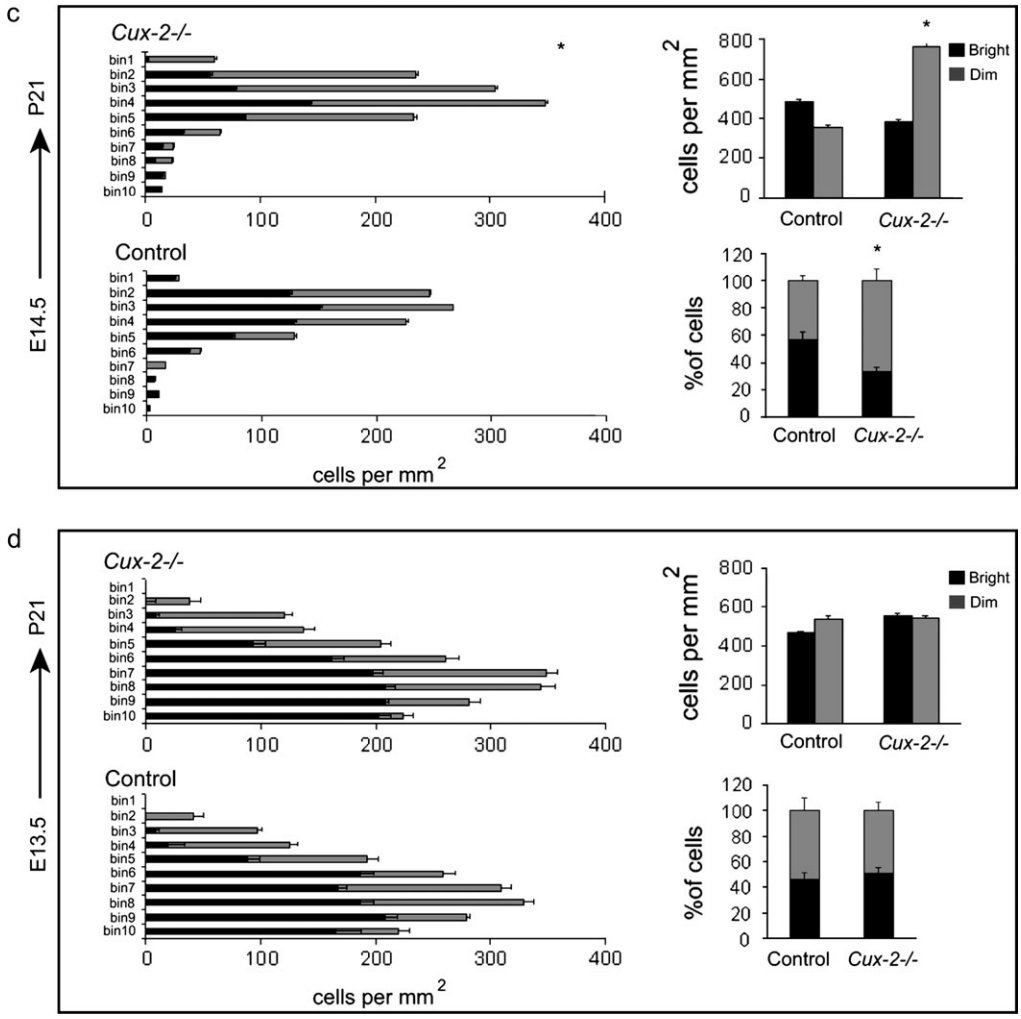

Figure 3. Continued.

analysis of the number of Tbr-2 and pH3 in the SVZ of E14.5 revealed increments of proliferating SVZ cells in E14.5 *Cux-2–/–* mice compared with WT animals. In contrast, no differences were found on cortical basal mitosis at E12.5, when lower layer neurons are generated (Supplementary Fig. 3).

Cux-2 Regulates the Number of Upper Cortical Neurons Independently of Cux-1

VZ and SVZ cells express low levels of Cux-1 protein, which also shows persistent expression in upper layer neurons (Nieto et al. 2004). To investigate the possibility that *Cux-1* and *Cux-2* might show redundant or interacting roles, we examined *Cux-1–/–; Cux-2–/–* double-mutant mice. This double gene deletion is embryonically lethal for reasons that are still undetermined. The lethality of *Cux-1–/–; Cux-2–/–* double mutation is due to defects manifest at early embryonic stages (between E9 and E15) (Cubelos B and Nieto M., unpublished data). However, although this phenotype is highly penetrant, a small proportion of mice develop to birth. Nissl staining of P0 coronal sections showed no gross abnormalities in the double and single *Cux-1* and *Cux-2* mutants and their cortex appeared to be normally laminated (Fig. 6*a*). We analyzed the migration and the number of E16.5 BrdU-labeled neurons at birth (P0) in *Cux-1–/–; Cux-2–/–* double mutants, compared with single *Cux-2-/-* mutants, and control littermates (Fig. 6*b,c*). The migration patterns of BrdU-labeled cells to the upper layer of the cortex were indistinguishable in all genotypes. However, the number of E16.5-birthdated neurons was significantly increased in the cortex of *Cux-1–/–; Cux-2–/–* double-mutant mice compared with controls, but this increase was no greater than that observed in the *Cux-2* single-mutant mice (Fig. 6*c*). These experiments rule out the possibility that an unrepressed function of *Cux-1* is responsible for the increased proliferation of upper layer neurons in *Cux-2* mutant mice. They moreover provide evidence that the control of upper layer neuron number is a unique function of *Cux-2* and is not redundant with *Cux-1* activities.

Cux-2 Controls Reentry of Precursor Cells into the Cell Cycle in a Cell-Autonomous Manner

The higher number of weakly BrdU-labeled cells in the cortex of *Cux-2–/–* mice suggested that neuronal precursors in these animals underwent more cell divisions than WT cells immediately before the generation of upper layer neurons. To investigate this further, we set out to unequivocally identify whether cortical neurons had been generated from precursors that had divided once, or more than once, by sequential

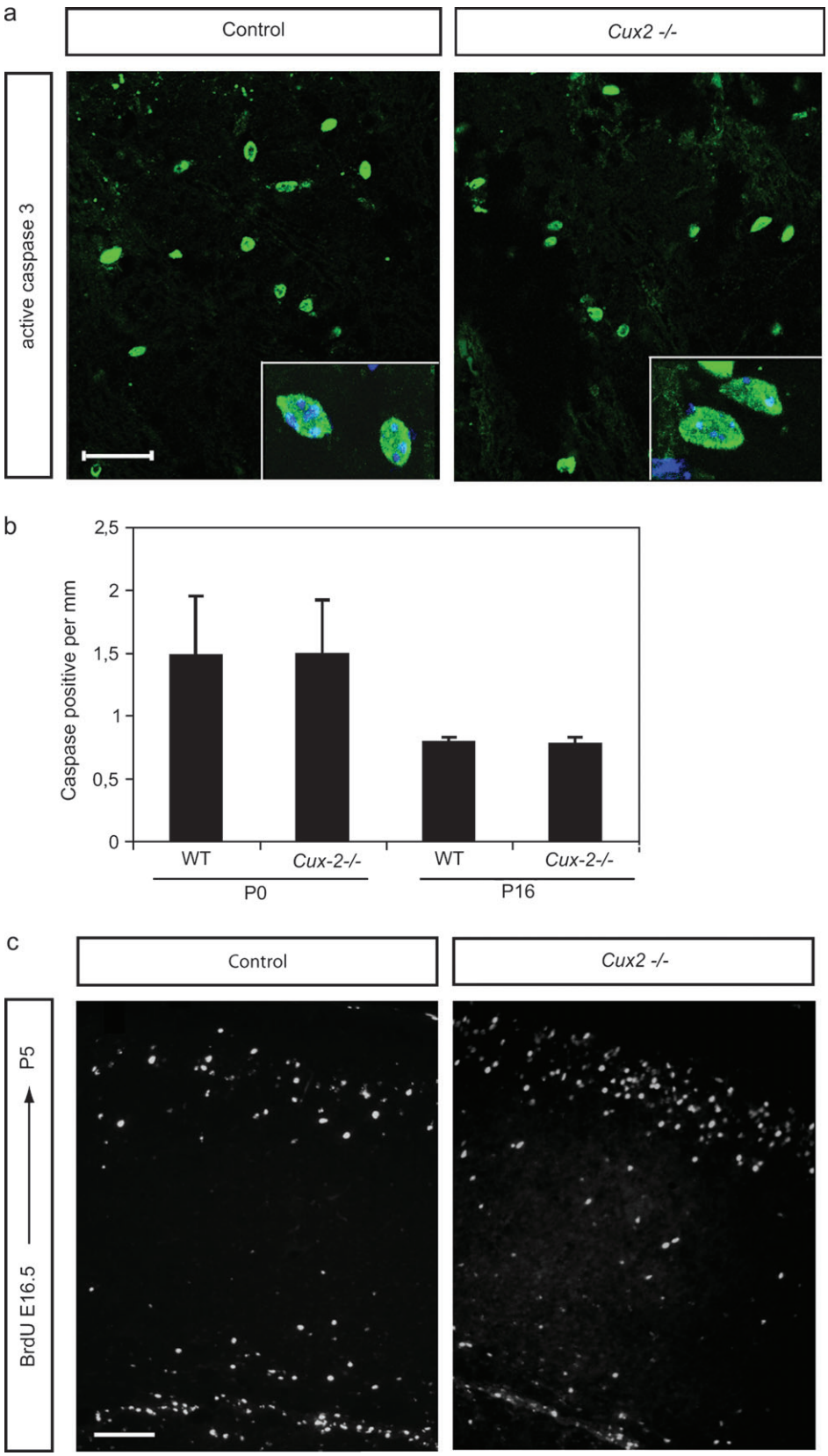

Figure 4. Brains of early postnatal *Cux-2−/−* mice contain an excess of upper cortical neurons that is not caused by decreased apoptosis. (*a*) Detection of apoptotic cells with antiactive caspase-3 antibody on cortical sections of P0 control and *Cux-2−/−* animals. Inset shows detail of caspase-3 positive cell. (*b*) Quantification of antiactive caspase-3 staining of cortical sections of P0 (left) and P16 (right) control and *Cux-2−/−* animals; no differences were detected at either stage. (*c*) E16.5-birthdated (BrdU-labeled) neurons in the P5 cortex of control and *Cux-2−/−* littermates. Bars represent 100 μm (*a*) and 25 μm (*c*).

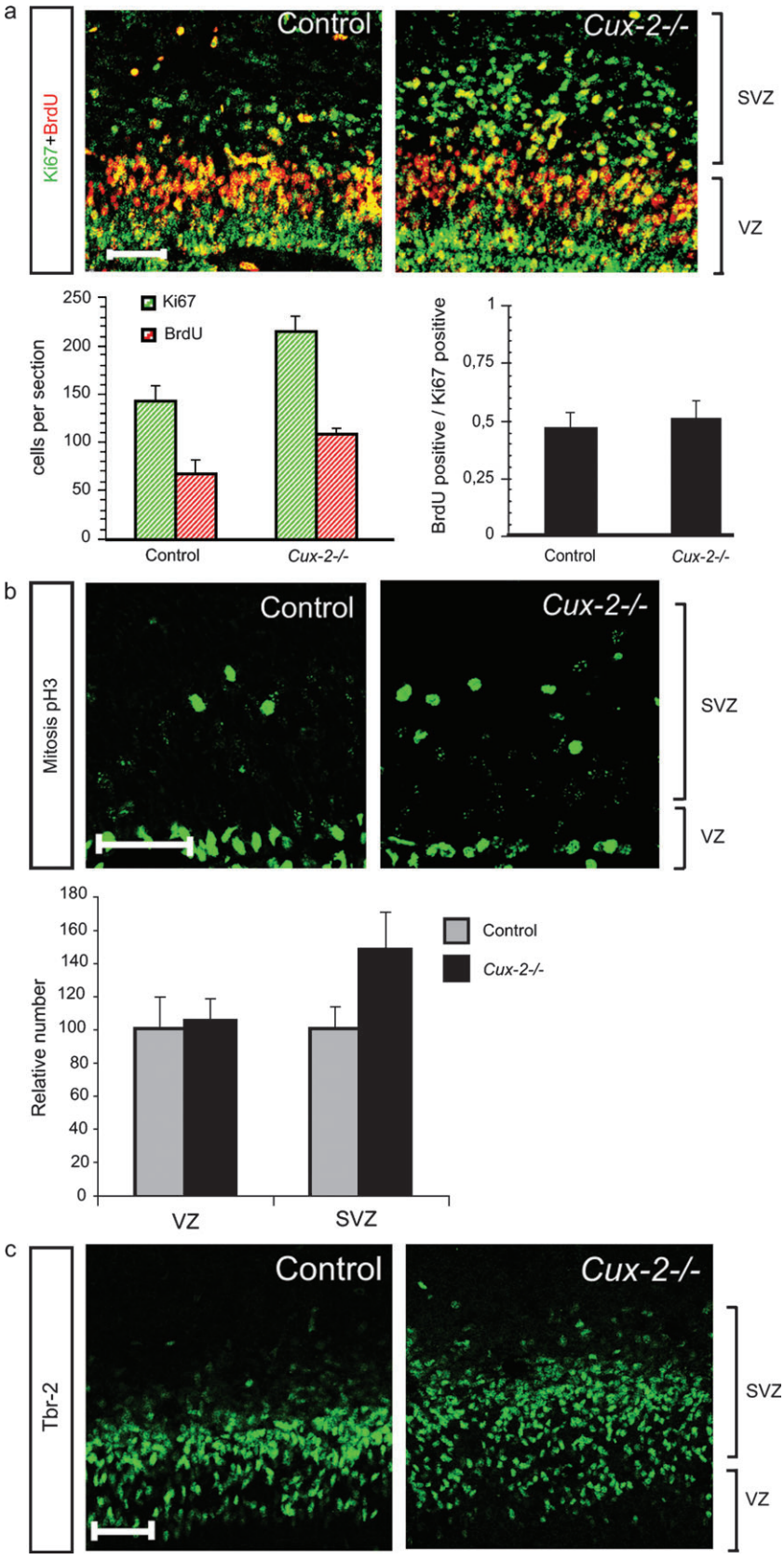

Figure 5. Proliferation is increased in the SVZ of *Cux-2*−/− mutant cortex. (*a*) Staining of Ki67, a protein expressed in all dividing cells (green), and BrdU-labeled dividing cells in S phase (red) after a 2-h pulse of the nucleotide in E15.5 cortical sections. The left-hand bar chart shows quantification of Ki67-positive and BrdU-positive cells ($n = 3$). The right-hand chart shows the proportion of dividing cells in S phase (BrdU positive) (number of BrdU+/number of Ki67+) in control and *Cux-2*−/− littermates ($n = 3$). (*b*) Detection of cortical pH3-positive cells undergoing mitosis at E15.5. The chart shows the relative numbers of mitotic cells in the VZ and SVZ of *Cux-2*−/− and control littermates, with the number of cells in the control mice set at 100%. Bar represents 50 μm (*a* and *b*). (*c*) Immunodetection of Tbr-2 positive cells in the SVZ of E15.5 cortical sections.

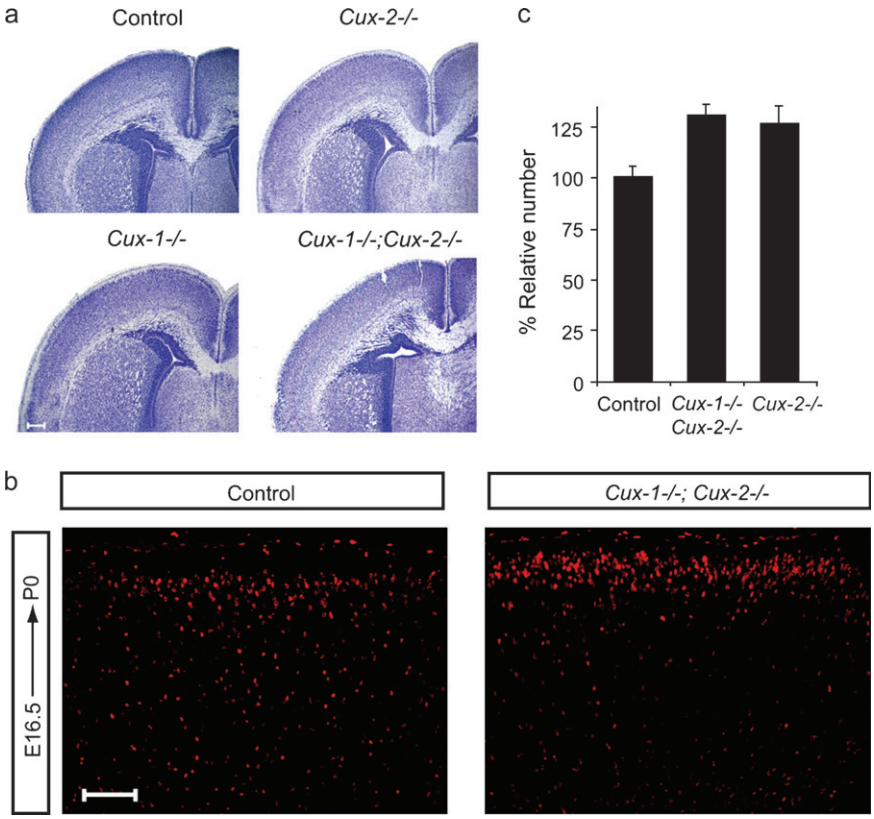

Figure 6. Analysis of the E16.5-birthdated neuronal population in *Cux-1; Cux-2* double-mutant mice. (*a*) Nissl staining of coronal sections of the telencephalon of control (*Cux-2*+/?), *Cux-2*−/−, and *Cux-1; Cux-2* double-mutant mice at P0. (*b*) Micrographs show staining of E16.5-birthdated (BrdU stained) neurons in sections of the P0 cortex of control and *Cux-1; Cux-2* double-mutant mice. (*c*) The chart shows the percentage (relative to control animals) of E16.5-birthdated neurons in the P0 cortex of control, *Cux-1; Cux-2* double mutant, and *Cux-2*−/− animals. Bars represent 500 μm (*a*) and 100 μm (*b*).

injection with 2 different halogenated nucleotide analog. The nucleotide analog IdU was given in a first injection, and CldU was injected 10 h later. The interval between injections allows many cells to exit the S phase after the first nucleotide injection but is shorter than the whole cell cycle, ensuring that cells reentering the cell cycle are labeled with the second nucleotide. Thus, cells that exited the cell cycle after the first injection are labeled with IdU only, whereas cells generated after subsequent subdivisions are double labeled with IdU and CldU (see diagram Fig. 7*c*). Cells that were not in the S phase at the first injection, or that diluted any incorporated IdU sufficiently during successive divisions, appear labeled only with CldU. We analyzed the upper layer neurons labeled at E14.5 in postnatal (P21) brain sections of control and *Cux-2*–/– animals (Fig. 7), and we found that the number of double-positive cells was much greater in the *Cux-2*–/– cortex (Fig. 7*a*). The ratio between the number of CldU-positive cells (second injection; red cells) and the total number of IdU-postive cells (first injection; green cells) shows that the proportion of precursor cells that reentered the cell cycle after the first injection was 2.5-fold higher in the *Cux-2*–/– mice than in control animals (Fig. 7*b*). Thus, our double-labeling analysis suggests that *Cux-2* controls exit from the cell cycle (Fig. 7*c*,*d*).

To investigate whether the phenotype of *Cux-2*-deficient precursors reflects a cell- or noncell-autonomous function, we overexpressed *Cux-2* in dividing embryonic neural stem cells grown as neurospheres in vitro. After cotransfection with *Cux-2*, or the empty vector (control), together with a GFP reporter, dissociated single GFP-positive cells were sorted by flow cytometry fluorescence activated cell sorting (FACS) (Fig. 7*e*). Sorted cells were then seeded at clonal density, and the number of neurospheres was quantified after 7 days in culture. As shown in Figure 7*f*,*g*, overexpression of *Cux-2* significantly reduced the number of neurospheres generated from the sorted cells, compared with control cells. Given that *Cux-2*-expressing cells and control cells were equally able to survive and differentiate into glia and neurons when plated in differentiating conditions (not shown), the reduced neurosphere formation by *Cux-2* overexpressing progenitors was not due to increased death rate or to changes in cell fate. These results therefore strongly suggest that *Cux-2* is able to direct cells out of the cell cycle in a cell-autonomous manner.

Discussion

In the present study, we demonstrate that expression of *Cux-2* selectively controls the proliferation of intermediate neuronal precursors in the SVZ and the number of upper layer neurons. In the context of evolution, the actions of *Cux-2* during development might provide mechanisms controlling the appearance and expansion of upper layer neurons.

Our data indicate that the restricted expression of *Cux-2* in the SVZ selectively controls the proliferation rates of neuronal intermediate precursors during mouse development. The role of *Cux-2* in cell cycle regulation was previously suggested by

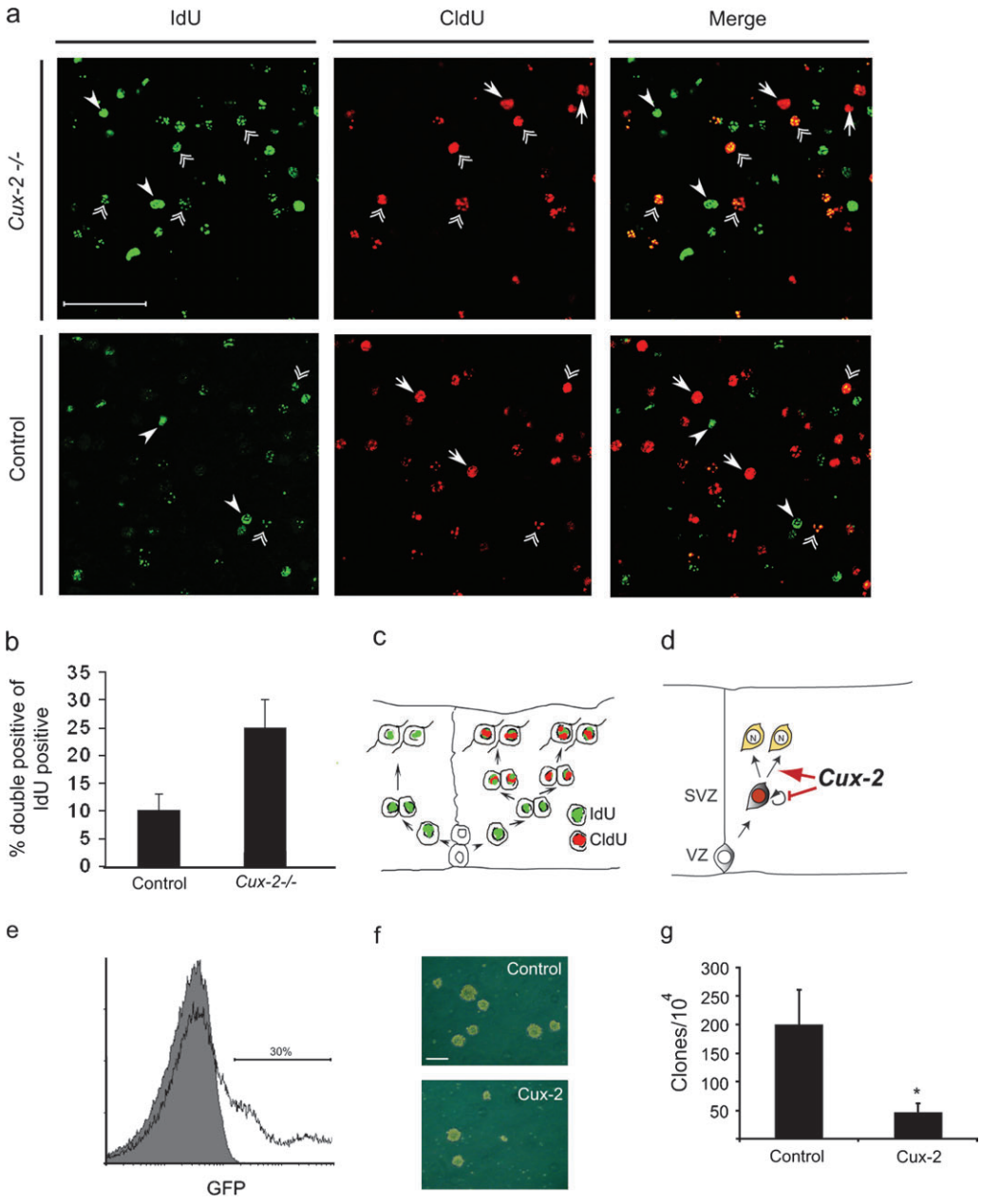

Figure 7. *Cux-2* regulates cell cycle exit. (*a*) Confocal images of neurons stained for IdU (green) and CldU (red) in cortical sections of the brains of P21 WT and *Cux-2*−/− mice that had been sequentially injected with the nucleotides at E14.5 (IdU, first injection; CldU, second injection: 10-h interval). Arrowheads mark single-labeled IdU-positive cells. Arrows mark single-labeled CldU-positive cells. Double-labeled cells (yellow on merged panel, double arrows) identify neurons generated from precursor cells that underwent 2 or more rounds of division after the initial injection with IdU. Bar represents 50 μm. (*b*) Double-positive cells (IdU+ and CldU+) as a percentage of the total number of IdU+ cells in control and *Cux-2*-deficient mice, providing an estimate of the proportion of neurons generated from precursors that reentered the cell cycle after the initial IdU injection. $^*P < 0.01$. (*c*) Schematic representation of the experimental design. (*d*) *Cux-2* may promote reentry of SVZ precursors into the cell cycle (N, neuron). The cell with red nucleus represents proliferating SVZ precursors. (*e*) Flow cytometry histogram of cells nucleotransfected with *Cux-2* and a GFP reporter. (*f*) Micrographs showing neurospheres after 10 days in culture by GFP-positive cells cotransfected with a DNA construct expressing *Cux-2* or the empty vector. Bar represents 100 μm. (*g*) Neurospheres formation as a proportion of total cells plated. $^*P < 0.01$ ($n = 3$).

its reported expression in tissues undergoing extended proliferation during embryonic development such as the limb bud progress zones or the urogenital system (Iulianella et al. 2003) but has not been demonstrated before. Hence, we herein provide the first evidence demonstrating a role for *Cux-2* in cell proliferation.

Interestingly, our studies demonstrate that *Cux-2* limits the number of times SVZ neuronal precursors go through the cell cycle. Our neuronal birthdating and double-labeling experiments demonstrate that *Cux-2*−/− upper layer precursors reenter the cell cycle at a higher frequency than their WT counterparts (Fig. 7*d*). Concurrently, we observed an expansion of intermediate neuronal precursors in the SVZ of the developing *Cux-2*−/− mice. This selective expansion is most definitively demonstrated by an increase in *Tbr-2*-expressing cells but no changes in precursors of the VZ. This selective

effect of *Cux-2* in SVZ cells supports the notion that the functions of *Cux-2* are cell autonomous. Cell-autonomous mechanisms are also strongly supported by our experiments showing that overexpression of *Cux-2* decreases proliferation in neural progenitor cells in vitro.

The increased numbers in the number of SVZ precursors in *Cux-2*–/– mice are quite significant (about 40% increment). This excessive proliferation temporally correlates with increased production of late-born neurons that migrate to the upper layers in normal patterns (30–40% in BrdU experiments). This causes parallel increments in cell density of layers II–IV (20–30% increment), as well as a moderate increase in upper layer thickness (15% increment).

Somewhat surprisingly, *Cux-2* does not appear to be functionally redundant with *Cux-1* in the SVZ precursor. The nonredundancy of *Cux-2* in intermediate neuronal precursors is suggested by its restricted expression in the SVZ, which is not shown by *Cux-1*, because it is expressed in VZ precursors as well. Our analysis of *Cux-1*–/–; *Cux-2*–/– double-mutant mice confirms this notion and demonstrates that the proliferation of upper layer neuronal precursor does not depend on *Cux-1* activity. The 2 *Cux* genes thus do not cooperate to control these aspects of neuronal development.

Our findings are of particular interest in the search for a mechanism to explain how the appearance and selective expansion of upper cortical layers during development evolved (Marin Padilla 2001; Hill and Walsh 2005; Kriegstein et al. 2006; Martinez-Cerdeno et al. 2006). A larger cortex implies that precursor cells undergo more rounds of division. In addition, the extended period of neurogenesis adds the upper layer to the cortex. Indeed, upper cortical layer neurons are highly represented in the primate cerebral cortex, especially in humans (reviewed in Hill and Walsh 2005). During development and evolution, inhibition of *Cux-2*-mediated cell cycle exit in the SVZ could be a target mechanism to expand the number of upper layer neurons without affecting the number of deep layer neurons. Thus, the functions of *Cux-2* fulfill both of the developmental and evolutionary necessities of expanding the number of layers. In this regard, evolution might have required *Cux-2* functions in processes such as the addition of upper layer neurons to the 3 layers of the reptilian cortex, the later selective expansion of upper layers in higher mammals (Reiner 1991; Marin Padilla 2001; Kriegstein et al. 2006), or the focal expansion of the upper layers and the SVZ that has been proposed to occur during the formation of the gyrencephalic cortex (Kriegstein et al. 2006).

Supplementary Material

Supplementary figures 1-3 can be found at: http://www.cercor.oxfordjournals.org/.

Funding

Ministerio de Educación y Ciencia (SAF2005-0094); Mutua Madrileña Automovilistica (2004); RYC-2003-006143 to M.N.; JdC-05-162-74c to B.C.; the Ministerio de Educación y Ciencia (BES-2006-13901) to A.S.-S.; National Institute of Neurological Disorders and Stroke (2RO1 NS032457) to C.A.W.; the Spanish Ministry of Health and Consumer Affairs and the Pro-CNIC Foundation to Centro Nacional de Investigaciones Cardiovasculares.

Notes

We thank B. Alarcón, S. Bartlett, F. Guillemot, M. Mellado, J. M. Rodríguez-Frade, P. Bovolenta, M. Guzmán, and H. M. van Santen for critical reading of the manuscript and for their experimental advice. We thank A. Nepveu (McGill University, Canada) for the anti-*Cux-2* antibody, M. Sheng (Picower Institute, MIT, Cambridge, MA) for the Tbr-1 antiserum, and A. J. van Wijnen (University of Massachusetts Medical School, Worcester, MA) for the *Cux-1* mutant mice. We are grateful to S. Montalban, S. Gutierrez-Erlandsson, and D. Esteban for technical assistance. During the generation of the *Cux-2loxP* conditional mice, M.N. was a Lefler fellow in the laboratory of C.A.W. We are indebted to C.A.W. for allowing us to continue the project at the Centro Nacional de Biotecnología (Madrid, Spain). C.A.W. is an Investigator at the Howard Hughes Medical Institute. *Conflict of Interest*: None declared.

Address correspondence to Email: mnlopez@cnb.uam.es.

References

Aten JA, Stap J, Hoebe R, Bakker PJ. 1994. Application and detection of IdUrd and CldUrd as two independent cell-cycle markers. Methods Cell Biol. 41:317–326.

Blochlinger K, Bodmer R, Jan LY, Jan YN. 1990. Patterns of expression of cut, a protein required for external sensory organ development in wild-type and cut mutant Drosophila embryos. Genes Dev. 4:1322–1331.

Bodmer R, Barbel S, Sheperd S, Jack JW, Jan LY, Jan YN. 1987. Transformation of sensory organs by mutations of the cut locus of D. melanogaster. Cell. 51:293–307.

Bulfone A, Smiga SM, Shimamura K, Peterson A, Puelles L, Rubenstein JL. 1995. T-brain-1: a homolog of Brachyury whose expression defines molecularly distinct domains within the cerebral cortex. Neuron. 15:63–78.

Calegari F, Haubensak W, Haffner C, Huttner WB. 2005. Selective lengthening of the cell cycle in the neurogenic subpopulation of neural progenitor cells during mouse brain development. J Neurosci. 25:6533–6538.

Cappello S, Attardo A, Wu X, Iwasato T, Itohara S, Wilsch-Brauninger M, Eilken HM, Rieger MA, Schroeder TT, Huttner WB, et al. 2006. The Rho-GTPase cdc42 regulates neural progenitor fate at the apical surface. Nat Neurosci. 9:1099–1107.

Chenn A, Walsh CA. 2002. Regulation of cerebral cortical size by control of cell cycle exit in neural precursors. Science. 297:365–369.

Cubelos B, Gimenez C, Zafra F. 2005. Localization of the GLYT1 glycine transporter at glutamatergic synapses in the rat brain. Cereb Cortex. 15:448–459.

Englund C, Fink A, Lau C, Pham D, Daza RA, Bulfone A, Kowalczyk T, Hevner RF. 2005. Pax6, Tbr2, and Tbr1 are expressed sequentially by radial glia, intermediate progenitor cells, and postmitotic neurons in developing neocortex. J Neurosci. 25:247–251.

Ferland RJ, Cherry TJ, Preware PO, Morrisey EE, Walsh CA. 2003. Characterization of Foxp2 and Foxp1 mRNA and protein in the developing and mature brain. J Comp Neurol. 460:266–279.

Gingras H, Cases O, Krasilnikova M, Berube G, Nepveu A. 2005. Biochemical characterization of the mammalian Cux2 protein. Gene. 344:273–285.

Glickstein SB, Alexander S, Ross ME. 2007. Differences in cyclin D2 and D1 protein expression distinguish forebrain progenitor subsets. Cereb Cortex. 17:632–642.

Gotz M, Huttner WB. 2005. The cell biology of neurogenesis. Nat Rev Mol Cell Biol. 6:777–788.

Grueber WB, Jan LY, Jan YN. 2003. Different levels of the homeodomain protein cut regulate distinct dendrite branching patterns of Drosophila multidendritic neurons. Cell. 112:805–818.

Guillemot F, Molnar Z, Tarabykin V, Stoykova A. 2006. Molecular mechanisms of cortical differentiation. Eur J Neurosci. 23:857–868.

Haubensak W, Attardo A, Denk W, Huttner WB. 2004. Neurons arise in the basal neuroepithelium of the early mammalian telencephalon: a major site of neurogenesis. Proc Natl Acad Sci USA. 101:3196–3201.

Hevner RF, Shi L, Justice N, Hsueh Y, Sheng M, Smiga S, Bulfone A, Goffinet AM, Campagnoni AT, Rubenstein JL. 2001. Tbr1 regulates differentiation of the preplate and layer 6. Neuron. 29:353–366.

Hill RS, Walsh CA. 2005. Molecular insights into human brain evolution. Nature. 437:64–67.

Iulianella A, Vanden Heuvel G, Trainor P. 2003. Dynamic expression of murine Cux2 in craniofacial, limb, urogenital and neuronal primordia. Gene Expr Patterns. 3:571–577.

Kriegstein A, Noctor S, Martinez-Cerdeno V. 2006. Patterns of neural stem and progenitor cell division may underlie evolutionary cortical expansion. Nat Rev Neurosci. 7:883–890.

Luong MX, van der Meijden CM, Xing D, Hesselton R, Monuki ES, Jones SN, Lian JB, Stein JL, Stein GS, Neufeld EJ, et al. 2002. Genetic ablation of the CDP/Cux protein C terminus results in hair cycle defects and reduced male fertility. Mol Cell Biol. 22: 1424–1437.

Malatesta P, Hartfuss E, Gotz M. 2000. Isolation of radial glial cells by fluorescent-activated cell sorting reveals a neuronal lineage. Development. 127:5253–5263.

Marin Padilla M. 2001. [The evolution of the structure of the neocortex in mammals: a new theory of cytoarchitecture]. Rev Neurol. 33:843–853.

Martinez-Cerdeno V, Noctor SC, Kriegstein AR. 2006. The role of intermediate progenitor cells in the evolutionary expansion of the cerebral cortex. Cereb Cortex. 16(Suppl 1):i152–i161.

McEvilly RJ, de Diaz MO, Schonemann MD, Hooshmand F, Rosenfeld MG. 2002. Transcriptional regulation of cortical neuron migration by POU domain factors. Science. 295:1528–1532.

Miyata T, Kawaguchi A, Saito K, Kawano M, Muto T, Ogawa M. 2004. Asymmetric production of surface-dividing and non-surface-dividing cortical progenitor cells. Development. 131:3133–3145.

Nieto M, Monuki ES, Tang H, Imitola J, Haubst N, Khoury SJ, Cunningham J, Gotz M, Walsh CA. 2004. Expression of Cux-1 and Cux-2 in the subventricular zone and upper layers II-IV of the cerebral cortex. J Comp Neurol. 479:168–180.

Noctor SC, Flint AC, Weissman TA, Dammerman RS, Kriegstein AR. 2001. Neurons derived from radial glial cells establish radial units in neocortex. Nature. 409:714–720.

Noctor SC, Martinez-Cerdeno V, Ivic L, Kriegstein AR. 2004. Cortical neurons arise in symmetric and asymmetric division zones and migrate through specific phases. Nat Neurosci. 7:136–144.

Nowakowski RS, Caviness VS, Jr., Takahashi T, Hayes NL. 2002. Population dynamics during cell proliferation and neuronogenesis in the developing murine neocortex. Results Probl Cell Differ. 39:1–25.

Paxinos G, Watson C. 1982. The rat brain in stereotaxis coordinates. New York: Academic Press.

Quaggin SE, Heuvel GB, Golden K, Bodmer R, Igarashi P. 1996. Primary structure, neural-specific expression, and chromosomal localization of Cux-2, a second murine homeobox gene related to Drosophila cut. J Biol Chem. 271:22624–22634.

Reiner A. 1991. A comparison of neurotransmitter-specific and neuropeptide-specific neuronal cell types present in the dorsal cortex in turtles with those present in the isocortex in mammals: implications for the evolution of isocortex. Brain Behav Evol. 38:53–91.

Rubenstein JL, Anderson S, Shi L, Miyashita-Lin E, Bulfone A, Hevner R. 1999. Genetic control of cortical regionalization and connectivity. Cereb Cortex. 9:524–532.

Sterio DC. 1984. The unbiased estimation of number and sizes of arbitrary particles using the disector. J Microsc. 134:127–136.

Sugitani Y, Nakai S, Minowa O, Nishi M, Jishage K, Kawano H, Mori K, Ogawa M, Noda T. 2002. Brn-1 and Brn-2 share crucial roles in the production and positioning of mouse neocortical neurons. Genes Dev. 16:1760–1765.

Takahashi T, Nowakowski RS, Caviness VS, Jr. 1995. The cell cycle of the pseudostratified ventricular epithelium of the embryonic murine cerebral wall. J Neurosci. 15:6046–6057.

Tarabykin V, Stoykova A, Usman N, Gruss P. 2001. Cortical upper layer neurons derive from the subventricular zone as indicated by Svet1 gene expression. Development. 128:1983–1993.

Wu SX, Goebbels S, Nakamura K, Kometani K, Minato N, Kaneko T, Nave KA, Tamamaki N. 2005. Pyramidal neurons of upper cortical layers generated by NEX-positive progenitor cells in the subventricular zone. Proc Natl Acad Sci USA. 102:17172–17177.

Zimmer C, Tiveron MC, Bodmer R, Cremer H. 2004. Dynamics of Cux2 expression suggests that an early pool of SVZ precursors is fated to become upper cortical layer neurons. Cereb Cortex. 14:1408–1420.